Title
Differences in graph theory functional connectivity in left and right temporal lobe epilepsy

Journal
Epilepsy Research, 108(10)

ISSN
0896-6974

Authors
Chiang, Sharon
Stern, John M
Engel, Jerome
et al.

Publication Date
2014-12-01

DOI
10.1016/j.eplepsyres.2014.09.023

Peer reviewed

Epilepsy Research (2014) 108, 1770—1781

journal homepage: www.elsevier.com/locate/epilepsyres

Differences in graph theory functional connectivity in left and right temporal lobe epilepsy

Sharon Chiang[a,1], John M. Stern[b], Jerome Engel Jr.[b,c,d,e], Harvey S. Levin[f,g], Zulfi Haneef[h,i,*,1]

[a] Department of Statistics, Rice University, Houston, TX, USA
[b] Department of Neurology, University of California, Los Angeles, CA, USA
[c] Department of Neurobiology, University of California, Los Angeles, CA, USA
[d] Department of Psychiatry and Biobehavioral Sciences, University of California, Los Angeles, CA, USA
[e] The Brain Research Institute, University of California, Los Angeles, CA, USA
[f] Department of Physical Medicine, Baylor College of Medicine, Houston, TX, USA
[g] Michael E. DeBakey VA Medical Center, Houston, TX, USA
[h] Department of Neurology, Baylor College of Medicine, Houston, TX, USA
[i] Neurology Care Line, VA Medical Center, Houston, TX, USA

Received 4 June 2014; received in revised form 7 September 2014; accepted 20 September 2014
Available online 28 September 2014

KEYWORDS
Brain imaging;
Epilepsy;
Functional MRI;
Graph theory;
Functional reorganization

Summary
Purpose: To investigate lateralized differences in limbic system functional connectivity between left and right temporal lobe epilepsy (TLE) using graph theory.
Methods: Interictal resting state fMRI was performed in 14 left TLE patients, 11 right TLE patients, and 12 controls. Graph theory analysis of 10 bilateral limbic regions of interest was conducted. Changes in edgewise functional connectivity, network topology, and regional topology were quantified, and then left and right TLE were compared.
Results: Limbic edgewise functional connectivity was predominantly reduced in both left and right TLE. More regional connections were reduced in right TLE, most prominently involving reduced interhemispheric connectivity between the bilateral insula and bilateral hippocampi. A smaller number of limbic connections were increased in TLE, more so in left than in right TLE. Topologically, the most pronounced change was a reduction in average network betweenness centrality and concurrent increase in left hippocampal betweenness centrality in right TLE.

Abbreviations: TLE, temporal lobe epilepsy; fcMRI, functional connectivity MRI; DMN, default mode network; AAL, automated anatomical labeling; FWER, family wise error rate; AED, anti-epileptic drug; FDR, false discovery rate.

* Corresponding author at: Department of Neurology, Baylor College of Medicine, One Baylor Plaza, MS: NB302, Houston, TX 77030, USA. Tel.: +1 832 355 4044; fax: +1 713 798 7561.
E-mail addresses: zulfi.haneef@bcm.edu, zulfihaneef@gmail.com (Z. Haneef).
[1] These authors contributed equally to this work.

http://dx.doi.org/10.1016/j.eplepsyres.2014.09.023
0920-1211/Published by Elsevier B.V.

In contrast, left TLE exhibited a weak trend toward increased right hippocampal betweenness centrality, with no change in average network betweenness centrality.
Conclusion: Limbic functional connectivity is predominantly reduced in both left and right TLE, with more pronounced reductions in right TLE. In contrast, left TLE exhibits both edgewise and topological changes that suggest a tendency toward reorganization. Network changes in TLE and lateralized differences thereof may have important diagnostic and prognostic implications.
Published by Elsevier B.V.

Introduction

Temporal lobe epilepsy (TLE) is the most common epilepsy in adults and most common pharmaco-resistant epilepsy amenable to surgical treatment. However, surgery is not possible in about 30% of TLE patients, primarily due to a lack of clear localizing abnormality (Berg et al., 2003). In standard surgical evaluation protocols, high-resolution MRI and video-EEG play a central role (Duncan, 1997). Functional connectivity MRI (fcMRI) may provide an additionally potential useful technique to aid lateralization.

Structural and functional neuroimaging has shown that TLE is a disorder of altered brain networks involving both temporal and extratemporal changes (Chiang and Haneef, 2014; Engel et al., 2013; Spencer, 2002). In additional to temporal lobe structures (Bettus et al., 2010; Pittau et al., 2012), seizure-induced neuronal loss has been hypothesized to lead to reorganization of limbic connectivity (Spencer, 2002). Structural reorganization of the limbic system has been observed in TLE using diffusion tensor imaging, mostly involving the insula, superior temporal lobe, thalamus, and hippocampus (Bonilha et al., 2012).

Recent studies have found different patterns of functional connectivity between right and left TLE, including global functional impairment in right TLE and redistribution of functional activation in left TLE (Billingsley et al., 2001; Dupont et al., 2002; Vlooswijk et al., 2010). Other lateralized differences in subnetworks such as the default mode network (DMN) have also been identified (Haneef et al., 2012). A graph theoretic approach to investigating lateralized differences in TLE functional connectivity permits a network-level approach that can help elucidate pathophysiology (Chiang and Haneef, 2014). Additionally, characterization of the functional connectome using graph theoretic measures allows for quantification of connectomic differences which may potentially aid clinical lateralization.

In this study, we used a graph theoretic approach to analyze resting state fcMRI and characterize differences in limbic functional connectivity between left and right TLE compared to healthy controls. This consisted of three steps: (1) comparison of edgewise differences in functional connectivity, (2) comparison of whole-brain limbic network properties, and (3) comparison of network properties of limbic structures at a nodal level.

Materials and methods

Subjects

We studied 14 subjects with left TLE, 11 subjects with right TLE, and 12 controls. The study was approved by the Institutional Review Board for Baylor College of Medicine (BCM). Consenting patients were recruited from July 2011 to March 2014 from the BCM comprehensive epilepsy center following clinical evaluation, video-EEG monitoring, and high-resolution MR imaging. Patients with disabling cognitive impairment or other neurological co-morbidities were excluded. Control subjects were recruited through university advertisement and word-of-mouth, and were selected to match patient groups in age, gender, and educational background.

Image acquisition

Imaging was performed on a Philips Ingenia 3T MRI scanner (Philips Medical Systems, Best, Netherlands). Resting state fMRI was acquired axially for 10 min (TR = 6000 ms, TE = 30 ms, FOV = 228 mm, matrix = 100 × 100, slice thickness = 2.25 mm, 67 slices, 100 volumes). Subjects were instructed to lie still with eyes closed, and not asked to think about anything in particular during the functional sequence. Patients were requested not to fall asleep during imaging and were monitored by the imaging technician. T_1-weighted imaging was also performed as follows: TR = 2500 ms, TE = 4600 ms, FOV = 199 mm, matrix = 244 × 206, slice thickness = 1.4 mm, 284 slices.

fMRI preprocessing

Data pre-processing were performed using FSL (fMRIB Software Library) version 5.0.2 (Oxford, UK, www.fmrib.ox.ac.uk/fsl) (Forman et al., 1995; Woolrich et al., 2001). The first 12 s were discarded to attain magnetization equilibrium. Resting state functional images underwent non-brain tissue elimination (Smith, 2002); slice-timing correction; spatial smoothing using a Gaussian kernel (5 mm full-width half maximum); and co-registration to the T_1-weighted structural image. Common pre-processing steps for resting state fMRI were then applied, including temporal bandpass filtering ($0.01 < f < 0.1$ Hz) (Fox et al., 2005; Uddin et al., 2009) and removal of the following sources of spurious various using linear regression: six motion parameters and their temporal derivatives, ventricular signal, and white matter signal (Fox et al., 2005). Whole-brain signal regression was not performed, in order to increase test-retest reliability in graph theory analyses (Liang et al., 2012). Motion scrubbing was also performed (Power et al., 2012). Residuals were normalized prior to further analysis.

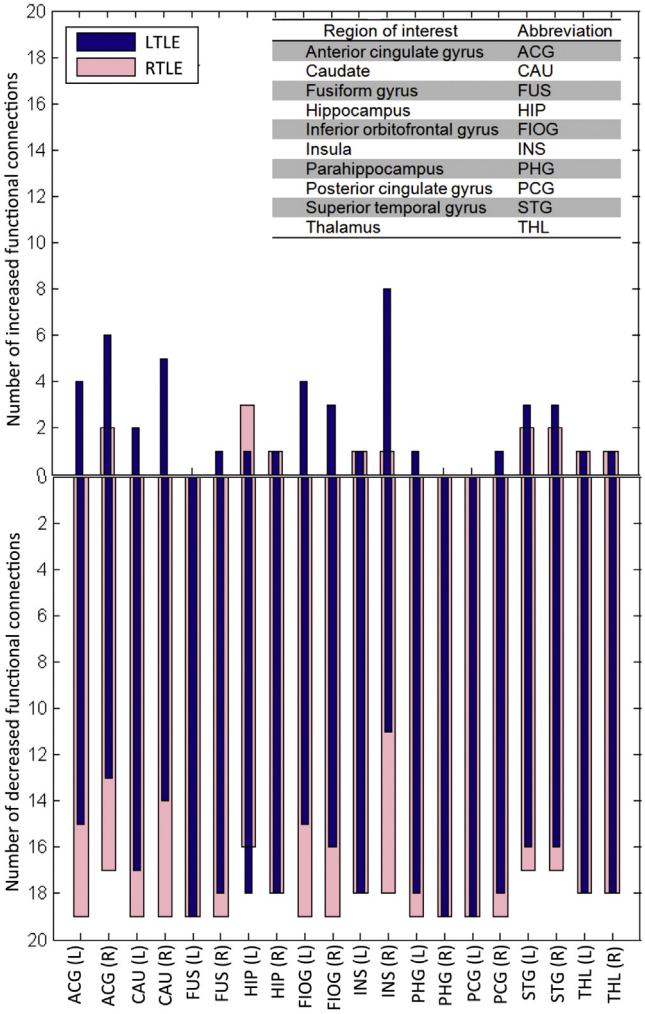

Figure 1 Histogram showing spatial distribution of increased/decreased limbic connectivity in LTLE and RTLE. Number of increased/decreased functional connections is shown on *y*-axis. LTLE, left TLE; RTLE, right TLE; L, left; R, right.

Limbic network functional connectivity

Statistical significance was evaluated at the 0.05 level. After registration to the MNI template image, functional connectivity was estimated between ten pairs of bilateral limbic and perilimbic regions of interest (regions in Fig. 1). These regions were chosen based on a priori knowledge, as they have consistently demonstrated structural changes in TLE (Keller and Roberts, 2008). Using the automated anatomical labeling (AAL) atlas (Tzourio-Mazoyer et al., 2002), regions of interest were first mapped to BOLD space. The representative time series for each region was obtained by averaging the fMRI residual time series across all voxels in the region. Functional connectivity was estimated through the Pearson correlation between all pairs of residual time series. Fisher's r-to-z transformation was applied to estimated correlation coefficients. To test for lateralized differences in the proportion of functional connections increased/decreased relative to controls, a two-sample two-sided test of equal proportions based on the raw connectivity matrix was performed. To identify limbic structures with connectivity most affected by TLE, structures with mean altered connectivity in the upper 15th percentile were reported. Non-parametric permutation testing with 1000 resamples was used to evaluate differences in functional connectivity for TLE compared to controls. To account for multiple comparisons, family wise Type 1 error rate (FWER) was controlled at the 0.05 level using the maximal statistic. This is considered the gold standard for accurately correcting for multiple testing (Westfall and Young, 1993) and was used to provide strong Type 1 error control. Nodes and edges were mapped onto cortical surfaces and visualized with the BrainNet Viewer (Fig. 2) (Xia et al., 2013).

Graph construction

Prior to graph construction, negative correlations were set to zero to improve the reliability of graph theory measures (Wang et al., 2011). Binary undirected graphs were constructed by thresholding the correlation matrix across a series of biologically plausible connection densities (Bullmore and Bassett, 2011), yielding a range of potential undirected graphs of the brain's functional network. This allowed comparison of network properties between patient subgroups and controls to reflect differences in connectome organization rather than differences in absolute connectivity.

Graph theory measures

Differences in functional reorganization between TLE subgroups were characterized based on graph theoretic measures of the functional connectome. A large number of functional topology measures can be calculated for brain networks, although of unclear relevance to TLE. Therefore, we chose to focus on basic measures of global functional topology studied previously (Bonilha et al., 2012), including average betweenness centrality, clustering coefficient, and global network efficiency. We examined these measures on a nodal level, including nodal betweenness centrality, clustering coefficient, and local efficiency (see Supplementary data).

Global and nodal graph theory measures were averaged across the non-random connection density range (Bullmore and Bassett, 2011) and compared to controls using non-parametric permutation testing with 1000 resamples. Multiple testing correction was performed by FWER control at the 0.05 level. Results are reported both before and after multiple testing correction. Statistical analyses were conducted using MATLAB version R2011a (MathWorks, Natick, Massachusetts, USA). Graph theory metrics were calculated using the Brain Connectivity Toolbox (Rubinov and Sporns, 2010).

Results

Patient details are in Table 1. We did not find a significant difference in patients with ipsilateral mesial temporal MRI findings (Fisher's exact p-value > 0.99), mesial temporal sclerosis (MTS) or hyperintense mesial signal (Fisher's exact

Table 1 Baseline characteristics for unilateral temporal lobe epilepsy patients.

Age (y)	Sex	Handedness	Epilepsy duration (years)	AEDs	Surgery	MRI findings	VEEG	PET	EEG	Neuropsychology memory dysfunction
33	F	R	16	CBZ, PHT	L ATL	L MTS	LT	Not done	LT sp	V > NV
23	F	R	4	LTG, PGB	No surgery	L MT fullness (CD or neoplasm)	LT	L MT hypometabolism	LT sp	V
22	F	R	4	LCM, LTG, TPM	L ATL	Normal	LT	Normal	LT slowing	V > NV
67	F	R	64	LEV	No surgery	L MTS	LT	Not done	BT sp	Not done
22	M	R	5	LEV, OXC	No surgery	Normal	LT	Normal	L FT sp	V > NV
23	F	R	11	FBM, ZNS	L ATL	L MT fullness (CD or neoplasm)	LT	Not done	LT sp, LF > RF sp	V + NV
39	F	R	27	LTG, ZNS, CBZ	No surgery	L MT hyperintensity	LT	Not done	LT > RT sp	Not done
32	M	R	17	CBZ, LEV	No surgery	Normal	LT	Not done	LT sp	V + NV
38	F	R	6	LTG, ZNS	No surgery	L MT hyperintensity	LT	Not done	LT sp	V + NV
37	F	R	22	LTG, CBZ, LCM	No surgery	Bilateral H hyperintensity	LT	Normal	BT/bifrontal sp	Not done
42	F	R	9	LTG	No surgery	L MT CD	LT	Not done	LT sp	Not done
33	F	R	12	LTG, LEV, AZ	No surgery	L MT CD	LT	Not done	LT sp	V > NV
28	M	L	2	LEV, OXC	No surgery	Normal	LT	Not done	LT sp	Normal
53	F	R	7	LTG	L ATL	L MT fullness (CD or neoplasm)	LT	LT hypometabolism	LT sp	Normal
47	F	R	3	LCM	No surgery	R MTS	RT	Not done	RT > LT sp	NV > V
36	M	L	30	LTG, ZNS	R ATL	Mild generalized parenchymal volume loss	RT	RT hypometabolism	RT sp	Not done
21	M	R	9	LCM, PHT	No surgery	Normal	RT	Not done	RT sp	Not done
28	M	R	6	LEV, LTG, TPM	No surgery	R H fullness/hyperintensity	RT	Not done	BT sp	V + NV
57	M	R	5	VPA, OXC	R ATL	R MTS	RT	Normal	RT sp	NV > V
37	M	R	27	LTG, CBZ	R ATL	R cavernous malformation	RT	Normal	RT > LT sp	NV

Table 1 (*Continued*)

Age (y)	Sex	Handedness	Epilepsy duration (years)	AEDs	Surgery	MRI findings	VEEG	PET	EEG	Neuropsychology memory dysfunction
49	F	R	48	LEV, LCM, RUF	No surgery	R MT hyperintensity/atrophy, L MT hyperintensity	RT	Not done	RT sp	V + NV
38	F	R	32	LEV, LTG	R ATL	R MTS	RT	Not done	RT sp	V + NV
61	F	R	56	LTG, PHT, VPA	No surgery	R MTS	RT	RT hypometabolism	RT sp	V > NV
56	M	R	56	LEV, VPA	No surgery	R H atrophy	RT	Not done	RT sp	V > NV
43	F	R	39	CBZ, LCM	No surgery	R H atrophy/hyperintensity	RT	Not done	RT > bifrontal sp	NV

AED, anti-epileptic drug; ATL, anterior temporal lobectomy; AZ, acetazolamide; BT, bitemporal; CBZ, carbamazepine; CD, cortical dysplasia; F, female; FBM, felbamate; FT, frontotemporal; H, hippocampus; L, left; LCM, lacosamide; LEV, levetiracetam; LF, left fronto-central; LT, left temporal; LTG, lamotrigine; M, male; MT, mesial temporal; MTS, mesial temporal sclerosis; NV, non-verbal; R, right; RF, right fronto-central; RT, right temporal; sp, spikes; OXC, oxcarbazepine; PGB, pregabalin; PHT, phenytoin; TPM, topiramate; V, verbal; VPA, valproic acid; ZNS, zonisamide.

p-value = 0.12), or normal MRI (Fisher's exact *p*-value = 0.34) between left and right TLE groups. Left TLE, right TLE, and control groups were similar in age (Kruskal–Wallis $\chi^2 = 4.26$, *p*-value = 0.119), gender (Pearson $\chi^2 = 4.40$, *p*-value = 0.111), and education (Kruskal–Wallis $\chi^2 = 3.76$, *p*-value = 0.15).

Limbic network functional connectivity

Most altered edgewise functional connections reflected decreases for both left and right TLE (Fig. 1). Increased functional connections were more often in left (23/190, or 12.1%) than right (7/190, or 3.7%) TLE (*p*-value = 0.004). Increases were mostly interhemispheric in left TLE and intrahemispheric in right TLE (Fig. 2a and b).

A larger number of significant changes in limbic edgewise connectivity were found in right than left TLE (Fig. 3d and e). Limbic structures with the most reduced connectivity (upper 15th percentile average altered connectivity) were the left posterior cingulate gyrus and bilateral thalami for left TLE, and the right hippocampus, right parahippocampus, and right posterior cingulate gyrus for right TLE. After multiple testing correction, significant reductions in functional connectivity included (1) the left and right hippocampus (*p*-value = 0.01) and (2) the left and right insula (*p*-value = 0.001) in right TLE (Fig. 3e, hatched squares).

Global functional topology

Fig. 4 compares average betweenness centrality, clustering coefficient, and global network efficiency across different levels of nonrandom connection densities. Patients with right TLE had significantly decreased levels of network betweenness centrality (*p*-value = 0.008). A trend toward decreased global efficiency of the left TLE limbic system was also identified prior to multiple testing correction. No other significant changes in network betweenness centrality, clustering coefficient, or global efficiency were observed. Average global network measurements are summarized in Table A.1.

Nodal functional topology

Fig. A.1 shows the overall spatial pattern of topological changes. The hippocampus and perihippocampal structures (parahippocampal gyrus, posterior cingulate gyrus, fusiform) generally exhibited decreases, with any increases being contralateral. The superior temporal gyrus mainly exhibited decreases. Deep gray matter structures (caudate, thalamus) mainly exhibited increases. Both increases and decreases were variably observed in frontal regions (inferior orbitofrontal gyrus, anterior cingulate gyrus). Clustering coefficient and local efficiency showed increases in left and decreases in right TLE, whereas betweenness centrality showed decreases in left and was variable in right TLE.

Of these changes, right TLE patients exhibited a significant increase in left hippocampal betweenness centrality, and decreases in betweenness centrality of the left insula and right parahippocampal gyrus. Local efficiency and clustering coefficient were decreased in the right hippocampus in both left and right TLE. In left TLE, the left superior

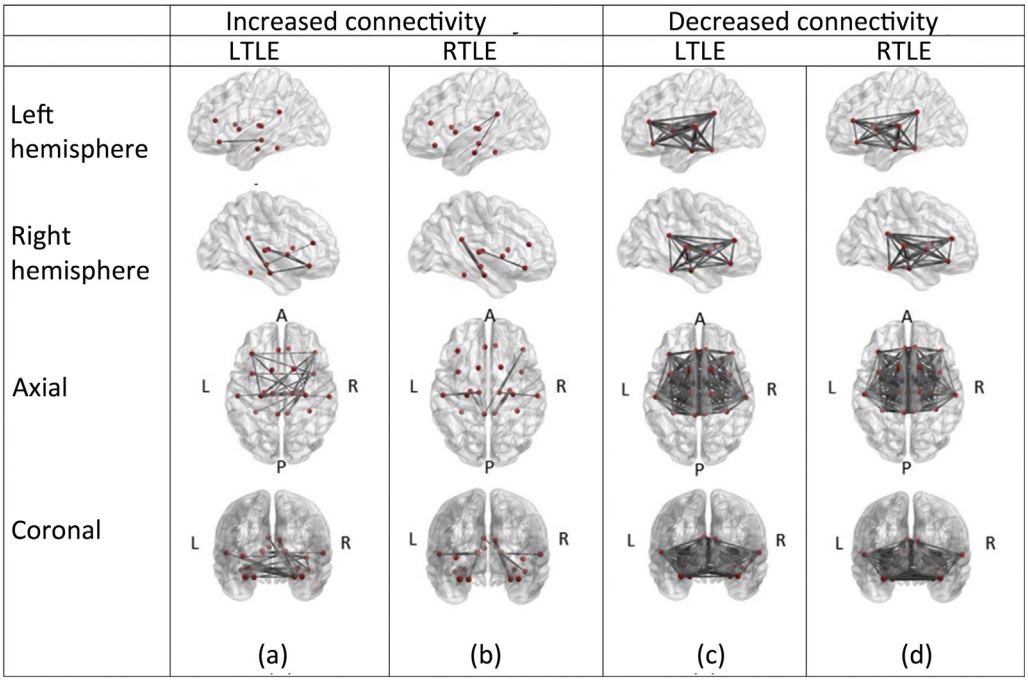

Figure 2 Increased (a—b) and decreased (c—d) functional connections in the limbic system for left and right TLE. LTLE, left TLE; RTLE, right TLE.

temporal gyrus exhibited decreases in local efficiency and nodal clustering coefficient. The left posterior cingulate gyrus also experienced decreased local efficiency in left TLE, along with a decrease in betweenness centrality of the left thalamus and a weak trend toward increased betweenness centrality of the right hippocampus prior to multiple testing correction. Outside of the hippocampus, all significant changes in local efficiency or clustering coefficient prior to multiple testing correction occurred in left TLE patients. After multiple testing correction, patients with right TLE exhibited a significant increase in betweenness centrality of the left hippocampus (p-value = 0.04) (Table 2).

Discussion

We investigated lateralized differences in the functional connectivity of the TLE limbic system. Limbic functional connectivity was predominantly reduced in both left and right TLE, with more pronounced reductions in right TLE. In contrast, left TLE exhibited changes in both edgewise connectivity and functional topology that suggest reorganization.

Limbic network functional connectivity

Using DTI, previous research has consistently demonstrated observations of structural fiber loss in the TLE limbic system (Bonilha et al., 2012; Riley et al., 2010). Our finding that functional connectivity is mainly reduced in TLE shows inter-modality agreement between DTI and fMRI. Additionally, we found that this reduction is more pronounced in right TLE, an observation corroborated by seed-based fcMRI analyses of the DMN (Haneef et al., 2012) and the limbic system (Doucet et al., 2013). Previous studies have found greater baseline levels of functional and structural connectivity in healthy brains in the left compared to right hemisphere (Barrick et al., 2007; Bettus et al., 2009). These greater baseline levels of left hemispheric connectivity may provide higher levels of functional and structural integrity which are protective against left-sided disease, resulting in the more pronounced reductions in connectivity for right TLE observed in our study.

Interestingly, we found that a larger proportion of limbic system connections were increased in left compared to right TLE. Consistent with this study, a similar trend of increased connectivity in left TLE compared to decreased connectivity in right TLE has also been observed in the DMN. In particular, increased connectivity of the anterior and posterior DMN has been observed in left TLE, whereas decreased connectivity of the posterior DMN has been observed in right TLE (Haneef et al., 2012). Our data provide evidence supporting the concept of functional redistribution in left TLE and bilateral functional impairment in right TLE (Billingsley et al., 2001; Dupont et al., 2002; Vlooswijk et al., 2010). This may reflect compensatory changes necessitated by greater cognitive deficits in left TLE (Mayeux et al., 1980), resulting in reorganization and less impairment from reductions in left TLE connectivity. Alternatively, this may also represent a maladaptive process leading to greater cognitive deficits in left TLE, as research increasingly supports the notion that upregulations in mesial temporal lobe connectivity are not functionally efficient (Voets et al., 2014). Further investigation is needed to improve understanding of circumstances under which these functional changes are compensatory or maladaptive (Saur and Hartwigsen, 2012; Voets et al., 2014).

Previous research has highlighted the prominence of changes in connectivity of the posterior cingulate gyrus,

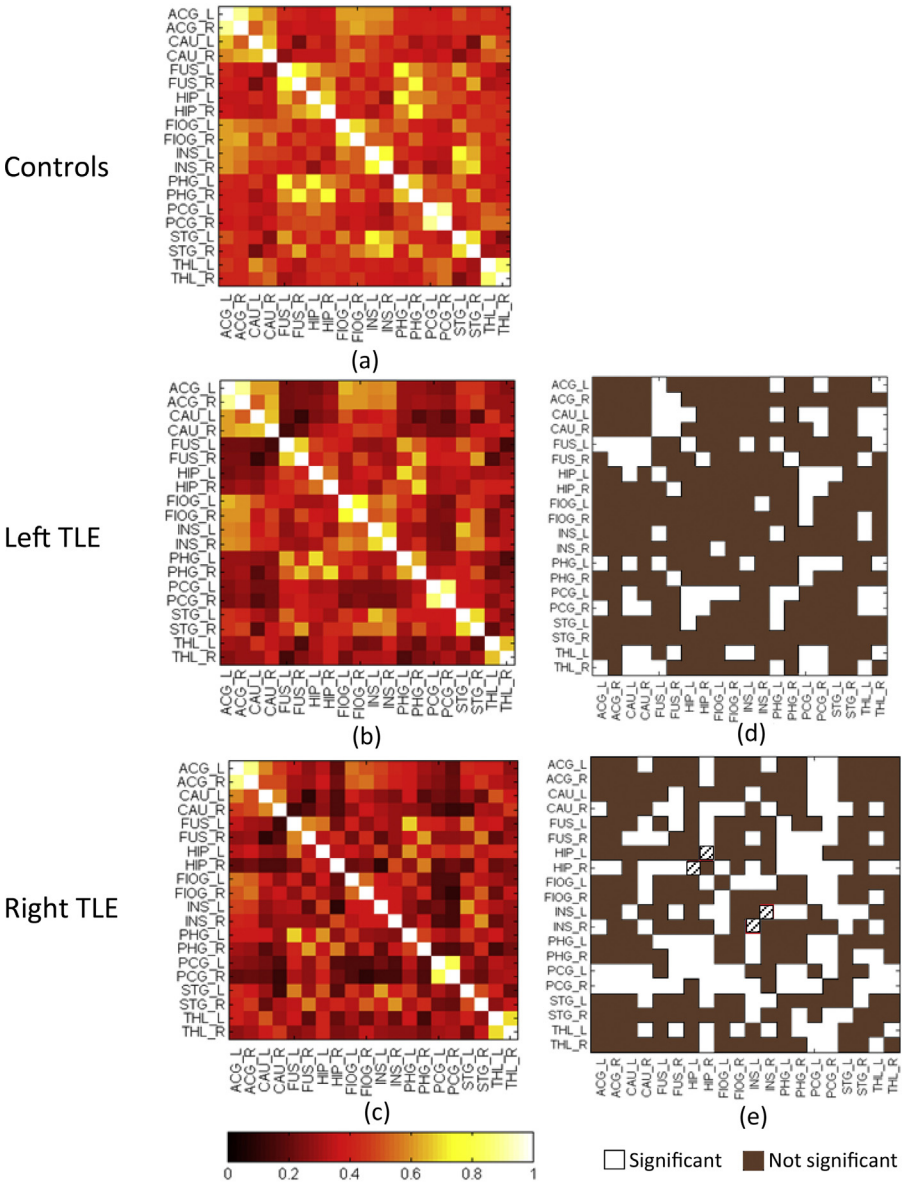

Figure 3 Edgewise functional connectivity of controls, left TLE, and right TLE patients. Mean correlation matrices for controls, left TLE, and right TLE are shown in (a–c). To provide an overview of groupwise differences, statistical significance prior to multiple testing correction is shown in matrices (d–e). For (a–c), the gradient (0–1) represents the edgewise Pearson correlation between pairs of limbic structures, with negative correlations set to 0. For (d–e), white and hatched squares indicate edgewise connections significantly different from controls prior to and after multiple testing correction, respectively. Abbreviations as listed in Fig. 1. L, left; R, right.

hippocampus, parahippocampus, insula, thalamus, and superior temporal gyrus in unilateral TLE (Bonilha et al., 2012; James et al., 2013; Liao et al., 2010). Here, we too found that these were the most affected structures in TLE. In addition, we show that edgewise connectivity of these structures are affected to different extents in left and right TLE, with the insula and parahippocampal gyrus most affected in right TLE, and the superior temporal gyrus and thalamus most affected in left TLE. The hippocampus and posterior cingulate were affected in both left and right TLE, similar to previous research (James et al., 2013), and is consistent with the selective vulnerability of functional connections between the hippocampal and posterior cingulate regions of the DMN identified in previous rs-fMRI studies (Voets et al., 2014).

Global and nodal functional topology

Prior examination of structural graph properties of the limbic network in TLE found no change in the overall efficiency of the limbic network when left and right TLE patients were evaluated as a single group (Bonilha et al., 2012). Here, we show that a trend toward decreased global efficiency of the limbic system in left TLE exists when left and right TLE patients are evaluated separately. This is

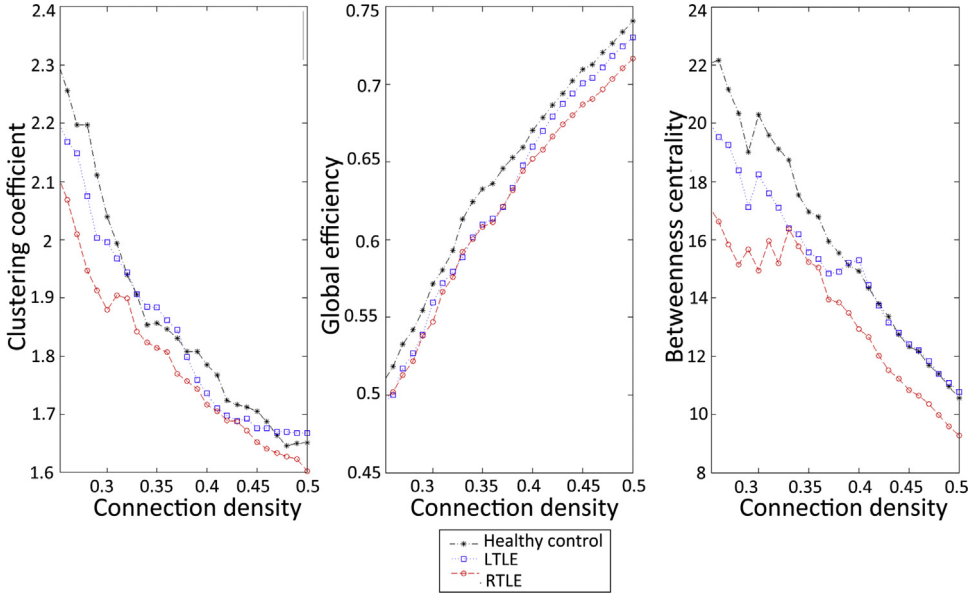

Figure 4 Network clustering coefficient, global efficiency, and betweenness centrality. Mean estimates across non-random connection density range (0.25—0.50) are shown. LTLE, left TLE; RTLE, right TLE.

supported by previous observations of decreased white matter global efficiency in left TLE when evaluated separately from right TLE (Liu et al., 2014). Clustering coefficient has variably been reported to be both increased (Bernhardt et al., 2011; Bonilha et al., 2012; Horstmann et al., 2010) and decreased (Liao et al., 2010; Vaessen et al., 2012; Vlooswijk et al., 2011) in TLE (Chiang and Haneef, 2014). In this study, clustering coefficient was not significantly

Table 2 Nodal functional measurements for healthy controls, left TLE, and right TLE. Values shown are *p*-values prior to multiple testing correction.

Region	Clustering coefficient		Local efficiency		Betweenness centrality	
	LTLE	RTLE	LTLE	RTLE	LTLE	RTLE
ACG L	0.11 ↑	0.39 ↓	0.11 ↑	0.42 ↓	0.06 ↓	0.20 ↓
ACG R	0.46 ↑	0.24 ↓	0.44 ↑	0.33 ↓	0.48 ↓	0.43 ↑
CAU L	0.44 ↑	0.37 ↑	0.48 ↓	0.27 ↑	0.23 ↑	0.36 ↑
CAU R	0.49 ↓	0.17 ↑	0.41 ↑	0.11 ↑	0.45 ↓	0.05 ↓
FUS L	0.34 ↓	0.46 ↑	0.26 ↓	0.42 ↑	0.49 ↓	0.24 ↑
FUS R	0.06 ↓	0.12 ↓	0.05 ↓	0.10 ↓	0.30 ↓	0.27 ↓
HIP L	0.43 ↓	0.29 ↓	0.37 ↓	0.39 ↓	0.49 ↓	**0.02** ↑
HIP R	**0.03** ↓	**0.04** ↓	**0.04** ↓	**0.02** ↓	0.09 ↑	0.22 ↓
FIOG L	0.09 ↑	0.32 ↓	0.05 ↑	0.26 ↓	0.29 ↓	0.09 ↓
FIOG R	0.18 ↑	0.35 ↓	0.19 ↑	0.25 ↓	0.31 ↓	0.21 ↓
INS L	0.34 ↓	0.51 ↑	0.24 ↓	0.36 ↓	0.26 ↑	**0.01** ↓
INS R	0.11 ↑	0.34 ↓	0.12 ↑	0.24 ↓	0.23 ↑	0.23 ↓
PHG L	0.37 ↓	0.24 ↑	0.30 ↓	0.36 ↑	0.16 ↓	0.11 ↓
PHG R	0.26 ↓	0.13 ↓	0.22 ↓	0.06 ↓	0.27 ↑	**0.02** ↓
PCG L	0.09 ↓	0.49 ↓	**0.04** ↓	0.42 ↓	0.07 ↓	0.12 ↓
PCG R	0.14 ↓	0.32 ↓	0.12 ↓	0.36 ↓	0.29 ↓	0.21 ↓
STG L	**0.04** ↓	0.11 ↓	**0.03** ↓	0.10 ↓	0.06 ↑	0.24 ↑
STG R	0.46 ↓	0.16 ↓	0.48 ↓	0.20 ↓	0.32 ↓	0.30 ↓
THL L	0.41 ↑	0.13 ↑	0.42 ↓	0.09 ↑	**0.05** ↓	0.41 ↑
THL R	0.45 ↑	0.28 ↑	0.47 ↑	0.19 ↑	0.35 ↓	0.47 ↑

Highlighted values are significantly different from controls prior (bold) and after (underlined) multiple testing correction at the 0.05 level.
↑ = increased relative to controls. ↓ = decreased relative to controls.
Abbreviations as per Fig. 1. L, left; LTLE, left TLE; R, right; RTLE, right TLE.

altered in TLE compared to controls. Although the reason for inter-study differences in clustering coefficient is not clear, heterogeneity in hippocampal sclerosis levels, sample size, age, and anti-epileptic drug (AED) regimens must be considered (Chiang and Haneef, 2014). Neuronal graph theory models of dentate gyrus sclerosis have shown that clustering coefficient increases during the majority of the sclerotic process and decreases in the final stages of sclerosis (Dyhrfjeld-Johnsen et al., 2007). Other factors, such as increased drug load, are also associated with decreases in clustering coefficient (Vlooswijk et al., 2011).

The most pronounced change in functional topology was a gain-of-function increase in betweenness centrality of the left hippocampus in right TLE, along with an overall decrease in network betweenness centrality. Table 2 suggests that the overall decrease in network betweenness centrality was attributable to decreases in nodal betweenness centrality throughout the limbic system, including the ipsilateral hippocampus (see also Fig. A.1). While not statistically significant individually, these combined to cause an overall decrease in network betweenness centrality. We postulate that the concomitant increase in left hippocampal betweenness centrality suggests a rerouting of ipsilateral hippocampal as well as other limbic system hubs to the contralateral hippocampus in right TLE. Observations of rerouted hubs involving the limbic system have also been noted in previous TLE research (Bernhardt et al., 2011; Liao et al., 2010; Liu et al., 2014).

In contrast, a much weaker increase in contralateral hippocampal betweenness centrality compared to controls was observed for left TLE. Our finding that the functional importance of the right hippocampus is only weakly increased in left TLE, compared to the marked increase in left hippocampal importance in right TLE, is supported by previous findings on the temporal precedence of cross-hippocampal functional connectivity in TLE. Although the contralateral hippocampus exerts influence over the ipsilateral hippocampus in both left and right TLE, the right hippocampus also exerts influence over the left hippocampus in healthy controls (Morgan et al., 2011), leading to less marked differences between controls and left TLE in right hippocampal influence. Increased functional activation of the contralateral hippocampus in response to memory cues has also been observed in right, but not left, TLE (Powell et al., 2007), suggesting that the contralateral hippocampus may be more plastic and able to assume lost functionality in right TLE. In light of the more disruptive connectivity changes in right TLE and compensatory changes in left TLE, an alternative hypothesis is that the greater compensatory response in left TLE leads to decreased need for the contralateral hippocampus to serve as a rerouted hub, whereas the more disruptive pattern in right TLE leads to a greater need for the contralateral hippocampus to serve as a rerouted hub. Higher functional adequacy of the left hippocampus in left TLE patients (Chelune, 1995) may also explain the ability of the left hippocampus to assume lost functionality from the remainder of the network.

Outside of the hippocampus, changes in clustering coefficient and local efficiency occurred only in left TLE. The greater prevalence of decreases in local efficiency in left TLE may reflect the greater cognitive deficits often clinically present in left TLE (Mayeux et al., 1980). However, whereas the right hippocampus exhibited decreases in clustering coefficient and local efficiency in right TLE, the left hippocampus was spared with respect to changes in clustering coefficient and local efficiency. Less pronounced changes in edgewise functional connectivity may be responsible for relative sparing in left TLE. Functional preservation of the left hippocampus may also be a mechanism to avoid cognitive deficits in left TLE. The observed interhemispheric pattern of increased functional connections in left TLE may contribute to left hippocampal preservation through increased connectivity to the contralateral intact hemisphere, offsetting decreases in clustering coefficient and local efficiency. In comparison, the majority of increased functional connections present in right TLE were intrahemispheric, with much fewer compensatory connections to the intact hemisphere.

Other than the right hippocampus, ipsilateral decreases in local efficiency of the posterior cingulate gyrus and superior temporal gyrus were observed for left TLE, with the most marked decrease in local efficiency observed in the ipsilateral superior temporal gyrus. Using structural data, decreases in left TLE local efficiency have also previously been found to occur primarily ipsilaterally, with the most marked reduction in left TLE local efficiency occurring in the left superior temporal gyrus (Liu et al., 2014).

This study has some limitations. Based on the moderate sample size of this study ($N = 37$), the differences identified in lateralized TLE limbic connectivity in this study warrant follow-up confirmatory studies based on larger samples. Another limitation is heterogeneity in AED usage and in underlying pathology, which may have affected connectivity differently. As functional connectivity often reflects structural integrity, functional connectivity would be expected to differ between patients with MTS or normal hippocampus on MRI. Although we did not find a difference in the proportions of patients with MTS or normal MRI between left and right TLE groups, our sample size was small, and these results need to be confirmed in larger studies. Heterogeneity in epilepsy duration and seizure frequency also complicate comparison of our results to previous fMRI studies of TLE. In particular, functional connectivity in epilepsy and other disorders involving limbic structures is increasingly recognized as a dynamic property which changes depending on the level of disease progression (Pitkanen and Sutula, 2002; Yao et al., 2014), relation to recent seizure activity (Jayakar et al., 2002), and treatment (Jansen et al., 2006; Vlooswijk et al., 2011). Variability in these factors may play a role in divergent results between fMRI studies on TLE. Within-subject resting state functional connectivity has also been found to exhibit less than expected reliability across and within scanning sessions. However, within-subject functional connectivity has been found to exhibit higher reliability among networks linked by structural connectivity (Honey et al., 2009), such as the limbic system explored in this study. There is increasing evidence that, while patterns of resting state functional connectivity may be constrained by a stable anatomical architecture, there is a level of within-subject variability in functional connectivity which is caused by dynamic changes in signal transmission time delays and local interactions between cells (Deco et al., 2011; Mehrkanoon et al., 2014).

In order to construct the nodes of subject-level graphs, we used the average time series across all voxels in a given

region. Averaging as a method of estimating a prototypical time course may not optimally reflect the most representative time course for all subjects equally. Additionally, a region of interest based approach was employed for defining the network examined in this study. Other data-driven approaches, such as independent component analysis, may allow for the extraction of other TLE networks while avoiding experimenter bias in the selection of seed regions. Approaches such as seed-based analyses and Granger causality offer alternative hypothesis-based approaches which do not require a priori knowledge of connectivity. Another important limitation is the choice of multiple comparisons adjustment. Whereas FWER was controlled in this study, false discovery rate (FDR) could have alternatively been controlled for less conservative statistical significance thresholds. However, increased power of FDR procedures comes at the cost of increased Type 1 error probability. Control of FWER thus may be considered a strength, by decreasing the probability that our results reflect false positives.

Conclusions

We identify several lateralized differences in the functional connectivity and graphical reorganization of the limbic network in TLE. We found that right TLE involves more pronounced reduction in limbic network connectivity and preliminary evidence that the right hippocampus is more vulnerable to loss of local functional connections in both left and right TLE. Preservation of the left hippocampus through interhemispheric increases in functional connectivity to the contralateral intact hemisphere may be a compensatory mechanism to avoid cognitive deficits in left TLE. These differences may help explain lateralized variations in neurobehavior and cognition. In addition, differences in graph theory measures provide potential quantitative markers of TLE laterality, disease severity, and prognosis, which are worthy of further investigation as a technique for TLE lateralization and disease monitoring.

Conflicts of interest

None of the authors has any conflict of interest to disclose. We confirm that we have read the Journal's position on issues involved in ethical publication and affirm that this report is consistent with those guidelines.

Acknowledgments

Sharon Chiang's contributions to this article include study concept or design, statistical analysis, drafting/revising the manuscript for content, and analysis/interpretation of data. John M. Stern's contributions to this article include interpreting results and revising the manuscript for content. Jerome Engel, Jr.'s contributions to this article include revising the manuscript for content. Harvey S. Levin's contributions to this article include revising the manuscript for content. Zulfi Haneef's contributions to this article include study concept or design, drafting/revising the manuscript for content, analysis/interpretation of data, study supervision, and obtaining funding. The authors thank Mr. Claudio Arena for his assistance in study participant recruitment.

Funding for design and conduct of this study; collection, management, analysis, and interpretation of the data; and preparation, review, or approval of the manuscript was provided by the Epilepsy Foundation of America. Support for this publication was provided by the National Library of Medicine Training Fellowship in Biomedical Informatics, Gulf Coast Consortia for Quantitative Biomedical Sciences (Grant #2T15LM007093-21) (SC); the National Institute of Health (Grant #5T32CA096520-07) (SC); the Leff Family Foundation (JMS); the National Institute of Neurological Disorders and Stroke (Grants #P01 NS02808, R01 NS33310, U01 NS42372, P20 NS80181) (JE); the Moody Foundation (HSL); Epilepsy Foundation of America (Research Grants Program) (ZH); and the Baylor College of Medicine Computational and Integrative Biomedical Research Center Seed Grant Awards (ZH).

Appendix A. Supplementary data

Supplementary data associated with this article can be found, in the online version, at http://dx.doi.org/10.1016/j.eplepsyres.2014.09.023.

References

Barrick, T.R., Lawes, I.N., Mackay, C.E., Clark, C.A., 2007. White matter pathway asymmetry underlies functional lateralization. Cereb. Cortex 17, 591—598.

Berg, A.T., Vickrey, B.G., Langfitt, J.T., Sperling, M.R., Walczak, T.S., Shinnar, S., Bazil, C.W., Pacia, S.V., Spencer, S.S., 2003. The multicenter study of epilepsy surgery: recruitment and selection for surgery. Epilepsia 44, 1425—1433.

Bernhardt, B.C., Chen, Z., He, Y., Evans, A.C., Bernasconi, N., 2011. Graph-theoretical analysis reveals disrupted small-world organization of cortical thickness correlation networks in temporal lobe epilepsy. Cereb. Cortex 21, 2147—2157.

Bettus, G., Bartolomei, F., Confort-Gouny, S., Guedj, E., Chauvel, P., Cozzone, P.J., Ranjeva, J.P., Guye, M., 2010. Role of resting state functional connectivity MRI in presurgical investigation of mesial temporal lobe epilepsy. J. Neurol. Neurosurg. Psychiatry 81, 1147—1154.

Bettus, G., Guedj, E., Joyeux, F., Confort-Gouny, S., Soulier, E., Laguitton, V., Cozzone, P.J., Chauvel, P., Ranjeva, J.P., Bartolomei, F., Guye, M., 2009. Decreased basal fMRI functional connectivity in epileptogenic networks and contralateral compensatory mechanisms. Hum. Brain Mapp. 30, 1580—1591.

Billingsley, R.L., McAndrews, M.P., Crawley, A.P., Mikulis, D.J., 2001. Functional MRI of phonological and semantic processing in temporal lobe epilepsy. Brain 124, 1218—1227.

Bonilha, L., Nesland, T., Martz, G.U., Joseph, J.E., Spampinato, M.V., Edwards, J.C., Tabesh, A., 2012. Medial temporal lobe epilepsy is associated with neuronal fibre loss and paradoxical increase in structural connectivity of limbic structures. J. Neurol. Neurosurg. Psychiatry 83, 903—909.

Bullmore, E.T., Bassett, D.S., 2011. Brain graphs: graphical models of the human brain connectome. Annu. Rev. Clin. Psychol. 7, 113—140.

Chelune, G.J., 1995. Hippocampal adequacy versus functional reserve: predicting memory functions following temporal lobectomy. Arch. Clin. Neuropsychol. 10, 413—432.

Chiang, S., Haneef, Z., 2014. Graph theory findings in the pathophysiology of temporal lobe epilepsy. Clin. Neurophysiol. 125, 1295–1305.

Deco, G., Jirsa, V.K., McIntosh, A.R., 2011. Emerging concepts for the dynamical organization of resting-state activity in the brain. Nat. Rev. Neurosci. 12, 43–56.

Doucet, G.E., Skidmore, C., Sharan, A.D., Sperling, M.R., Tracy, J.I., 2013. Functional connectivity abnormalities vary by amygdala subdivision and are associated with psychiatric symptoms in unilateral temporal epilepsy. Brain Cogn. 83, 171–182.

Duncan, J.S., 1997. Imaging and epilepsy. Brain 120, 339–377.

Dupont, S., Samson, Y., Van de Moortele, P.F., Samson, S., Poline, J.B., Hasboun, D., Le Bihan, D., Baulac, M., 2002. Bilateral hemispheric alteration of memory processes in right medial temporal lobe epilepsy. J. Neurol. Neurosurg. Psychiatry 73, 478–485.

Dyhrfjeld-Johnsen, J., Santhakumar, V., Morgan, R.J., Huerta, R., Tsimring, L., Soltesz, I., 2007. Topological determinants of epileptogenesis in large-scale structural and functional models of the dentate gyrus derived from experimental data. J. Neurophysiol. 97, 1566–1587.

Engel Jr., J., Thompson, P.M., Stern, J.M., Staba, R.J., Bragin, A., Mody, I., 2013. Connectomics and epilepsy. Curr. Opin. Neurol. 26, 186–194.

Forman, S.D., Cohen, J.D., Fitzgerald, M., Eddy, W.F., Mintun, M.A., Noll, D.C., 1995. Improved assessment of significant activation in functional magnetic resonance imaging (fMRI): use of a cluster-size threshold. Magn. Reson. Med. 33, 636–647.

Fox, M.D., Snyder, A.Z., Vincent, J.L., Corbetta, M., Van Essen, D.C., Raichle, M.E., 2005. The human brain is intrinsically organized into dynamic, anticorrelated functional networks. Proc. Natl. Acad. Sci. U. S. A. 102, 9673–9678.

Haneef, Z., Lenartowicz, A., Yeh, H.J., Engel Jr., J., Stern, J.M., 2012. Effect of lateralized temporal lobe epilepsy on the default mode network. Epilepsy Behav. 25, 350–357.

Honey, C.J., Sporns, O., Cammoun, L., Gigandet, X., Thiran, J.P., Meuli, R., Hagmann, P., 2009. Predicting human resting-state functional connectivity from structural connectivity. Proc. Natl. Acad. Sci. U. S. A. 106, 2035–2040.

Horstmann, M.T., Bialonski, S., Noennig, N., Mai, H., Prusseit, J., Wellmer, J., Hinrichs, H., Lehnertz, K., 2010. State dependent properties of epileptic brain networks: comparative graph-theoretical analyses of simultaneously recorded EEG and MEG. Clin. Neurophysiol. 121, 172–185.

James, G.A., Tripathi, S.P., Ojemann, J.G., Gross, R.E., Drane, D.L., 2013. Diminished default mode network recruitment of the hippocampus and parahippocampus in temporal lobe epilepsy. J. Neurosurg. 119, 288–300.

Jansen, J.F., Aldenkamp, A.P., Marian Majoie, H.J., Reijs, R.P., de Krom, M.C., Hofman, P.A., Eline Kooi, M., Nicolay, K., Backes, W.H., 2006. Functional MRI reveals declined prefrontal cortex activation in patients with epilepsy on topiramate therapy. Epilepsy Behav. 9, 181–185.

Jayakar, P., Bernal, B., Santiago Medina, L., Altman, N., 2002. False lateralization of language cortex on functional MRI after a cluster of focal seizures. Neurology 58, 490–492.

Keller, S.S., Roberts, N., 2008. Voxel-based morphometry of temporal lobe epilepsy: an introduction and review of the literature. Epilepsia 49, 741–757.

Liang, X., Wang, J., Yan, C., Shu, N., Xu, K., Gong, G., He, Y., 2012. Effects of different correlation metrics and preprocessing factors on small-world brain functional networks: a resting-state functional MRI study. PLoS ONE 7, e32766.

Liao, W., Zhang, Z., Pan, Z., Mantini, D., Ding, J., Duan, X., Luo, C., Lu, G., Chen, H., 2010. Altered functional connectivity and small-world in mesial temporal lobe epilepsy. PLoS ONE 5, e8525.

Liu, M., Chen, Z., Beaulieu, C., Gross, D.W., 2014. Disrupted anatomic white matter network in left mesial temporal lobe epilepsy. Epilepsia, 2014/03/22 ed.

Mayeux, R., Brandt, J., Rosen, J., Benson, D.F., 1980. Interictal memory and language impairment in temporal lobe epilepsy. Neurology 30, 120–125.

Mehrkanoon, S., Breakspear, M., Boonstra, T.W., 2014. Low-dimensional dynamics of resting-state cortical activity. Brain Topogr. 27, 338–352.

Morgan, V.L., Rogers, B.P., Sonmezturk, H.H., Gore, J.C., Abou-Khalil, B., 2011. Cross hippocampal influence in mesial temporal lobe epilepsy measured with high temporal resolution functional magnetic resonance imaging. Epilepsia 52, 1741–1749.

Pitkanen, A., Sutula, T.P., 2002. Is epilepsy a progressive disorder? Prospects for new therapeutic approaches in temporal-lobe epilepsy. Lancet Neurol. 1, 173–181.

Pittau, F., Grova, C., Moeller, F., Dubeau, F., Gotman, J., 2012. Patterns of altered functional connectivity in mesial temporal lobe epilepsy. Epilepsia 53, 1013–1023.

Powell, H.W., Richardson, M.P., Symms, M.R., Boulby, P.A., Thompson, P.J., Duncan, J.S., Koepp, M.J., 2007. Reorganization of verbal and nonverbal memory in temporal lobe epilepsy due to unilateral hippocampal sclerosis. Epilepsia 48, 1512–1525.

Power, J.D., Barnes, K.A., Snyder, A.Z., Schlaggar, B.L., Petersen, S.E., 2012. Spurious but systematic correlations in functional connectivity MRI networks arise from subject motion. Neuroimage 59, 2142–2154.

Riley, J.D., Franklin, D.L., Choi, V., Kim, R.C., Binder, D.K., Cramer, S.C., Lin, J.J., 2010. Altered white matter integrity in temporal lobe epilepsy: association with cognitive and clinical profiles. Epilepsia 51, 536–545.

Rubinov, M., Sporns, O., 2010. Complex network measures of brain connectivity: uses and interpretations. Neuroimage 52, 1059–1069.

Saur, D., Hartwigsen, G., 2012. Neurobiology of language recovery after stroke: lessons from neuroimaging studies. Arch. Phys. Med. Rehabil. 93, S15–S25.

Smith, S.M., 2002. Fast robust automated brain extraction. Hum. Brain Mapp. 17, 143–155.

Spencer, S.S., 2002. Neural networks in human epilepsy: evidence of and implications for treatment. Epilepsia 43, 219–227.

Tzourio-Mazoyer, N., Landeau, B., Papathanassiou, D., Crivello, F., Etard, O., Delcroix, N., Mazoyer, B., Joliot, M., 2002. Automated anatomical labeling of activations in SPM using a macroscopic anatomical parcellation of the MNI MRI single-subject brain. Neuroimage 15, 273–289.

Uddin, L.Q., Kelly, A.M., Biswal, B.B., Castellanos, F.X., Milham, M.P., 2009. Functional connectivity of default mode network components: correlation, anticorrelation, and causality. Hum. Brain Mapp. 30, 625–637.

Vaessen, M.J., Jansen, J.F., Vlooswijk, M.C., Hofman, P.A., Majoie, H.J., Aldenkamp, A.P., Backes, W.H., 2012. White matter network abnormalities are associated with cognitive decline in chronic epilepsy. Cereb. Cortex 22, 2139–2147.

Vlooswijk, M.C., Jansen, J.F., de Krom, M.C., Majoie, H.M., Hofman, P.A., Backes, W.H., Aldenkamp, A.P., 2010. Functional MRI in chronic epilepsy: associations with cognitive impairment. Lancet Neurol. 9, 1018–1027.

Vlooswijk, M.C., Vaessen, M.J., Jansen, J.F., de Krom, M.C., Majoie, H.J., Hofman, P.A., Aldenkamp, A.P., Backes, W.H., 2011. Loss of network efficiency associated with cognitive decline in chronic epilepsy. Neurology 77, 938–944.

Voets, N.L., Zamboni, G., Stokes, M.G., Carpenter, K., Stacey, R., Adcock, J.E., 2014. Aberrant functional connectivity in dissociable hippocampal networks is associated with deficits in memory. J. Neurosci. 34, 4920–4928.

Wang, J.H., Zuo, X.N., Gohel, S., Milham, M.P., Biswal, B.B., He, Y., 2011. Graph theoretical analysis of functional brain networks:

test-retest evaluation on short- and long-term resting-state functional MRI data. PLoS ONE 6, e21976.

Westfall, P.H., Young, S.S., 1993. Resampling-Based Multiple Testing: Examples and Methods for p-Value Adjustment. John Wiley & Sons, New York.

Woolrich, M.W., Ripley, B.D., Brady, M., Smith, S.M., 2001. Temporal autocorrelation in univariate linear modeling of FMRI data. Neuroimage 14, 1370—1386.

Xia, M., Wang, J., He, Y., 2013. BrainNet Viewer: a network visualization tool for human brain connectomics. PLOS ONE 8, e68910.

Yao, H., Zhou, B., Zhang, Z., Wang, P., Guo, Y., Shang, Y., Wang, L., Zhang, X., An, N., Liu, Y., 2014. Longitudinal alteration of amygdalar functional connectivity in mild cognitive impairment subjects revealed by resting-state FMRI. Brain Connect. 4, 361—370.